Title

The C677T Variant in MTHFR Modulates Associations Between Brain Integrity, Mood, and Cognitive Functioning in Old Age

Journal

Biological Psychiatry Cognitive Neuroscience and Neuroimaging, 2(3)

ISSN

2451-9022

Authors

Roussotte, Florence F
Hua, Xue
Narr, Katherine L
et al.

Publication Date

2017-04-01

DOI

10.1016/j.bpsc.2016.09.005

Peer reviewed

Archival Report

Biological Psychiatry: CNNI

The C677T Variant in *MTHFR* Modulates Associations Between Brain Integrity, Mood, and Cognitive Functioning in Old Age

Florence F. Roussotte, Xue Hua, Katherine L. Narr, Gary W. Small, and Paul M. Thompson, for the Alzheimer's Disease Neuroimaging Initiative

ABSTRACT

BACKGROUND: The C677T functional variant in the methylenetetrahydrofolate reductase (*MTHFR*) gene leads to reduced enzymatic activity and elevated blood homocysteine levels. Hyperhomocysteinemia has been linked with higher rates of cardiovascular diseases, cognitive decline, and late-life depression.

METHODS: Three-dimensional magnetic resonance imaging data were analyzed from 738 individuals (aged 75.5 ± 6.8 years; 438 men, 300 women), including 173 patients with Alzheimer's disease, 359 subjects with mild cognitive impairment, and 206 healthy older adults, scanned as part of the Alzheimer's Disease Neuroimaging Initiative.

RESULTS: We found that this variant associates with localized brain atrophy, after controlling for age, sex, and dementia status, in brain regions implicated in both intellectual and emotional functioning, notably the medial orbitofrontal cortices. The medial orbitofrontal cortex is involved in the cognitive modulation of emotional processes, and localized atrophy in this region was previously linked with both cognitive impairment and depressive symptoms. Here, we report that increased plasma homocysteine level mediates the association between *MTHFR* genotype and lower medial orbitofrontal volumes and that these volumes mediate the association between cognitive decline and depressed mood in this elderly cohort. We additionally show that vitamin B_{12} deficiency interacts with the C677T variant in the etiology of hyperhomocysteinemia.

CONCLUSIONS: This study sheds light on important relationships between vascular risk factors, age-related cognitive decline, and late-life depression, and it represents a significant advance in our understanding of clinically relevant associations relating to *MTHFR* genotype.

Keywords: Age-related cognitive decline, Brain atrophy, Homocysteine, Late-life depression, MRI, MTHFR

http://dx.doi.org/10.1016/j.bpsc.2016.09.005

Hyperhomocysteinemia, a metabolic anomaly involving elevated blood levels of the amino acid homocysteine, is associated with higher rates of numerous age-related disorders, such as cardiovascular diseases (1,2) including vascular dementia (3,4); cognitive decline (5–9); and depressed mood (10–12). Elevated plasma homocysteine levels may stem from the use of certain therapeutic drugs, from elevated alcohol ingestion, from intestinal malabsorption, or from impaired metabolism due to genetic alterations in metabolic enzymes, including methylenetetrahydrofolate reductase (MTHFR), most commonly when combined with insufficient dietary intake of B vitamins. Notably, homocysteine is recycled to methionine using vitamin B_{12} as a cofactor, and MTHFR, the rate-limiting enzyme in the methyl cycle, catalyzes the conversion of 5,10-methylenetetrahydrofolate to 5-methyltetrahydrofolate, a cosubstrate for homocysteine remethylation by methionine synthase. These relationships are illustrated in Figure 1.

We recently reported that older adults with higher homocysteine levels had more pronounced regional brain atrophy (13) and thinner cortical gray matter (14) on magnetic resonance imaging (MRI). We also found that the C677T variant in *MTHFR* was associated with smaller regional brain volumes in two independent elderly cohorts with mild cognitive impairment (MCI) (15). Increased susceptibility for cardiovascular diseases (16), which are strongly linked to both cognitive decline and depressive symptoms in old age (17), are also associated with the C677T variant.

Here, we first determined whether our previously reported associations between the T "risk" allele and more pronounced brain atrophy extended beyond individuals with MCI to both patients with dementia and healthy older adults. We further sought to model some of the mechanisms underlying relationships between brain integrity, clinical outcomes, and the genetic and environmental modulators of homocysteine metabolism. To this end, we first examined whether the effects of this *MTHFR* polymorphism on medial orbitofrontal volumes were mediated by its impact on plasma homocysteine levels. We also determined whether vitamin B_{12} deficiency influenced the strength of the relationship between this variant and homocysteine levels. We then found that lower cognitive

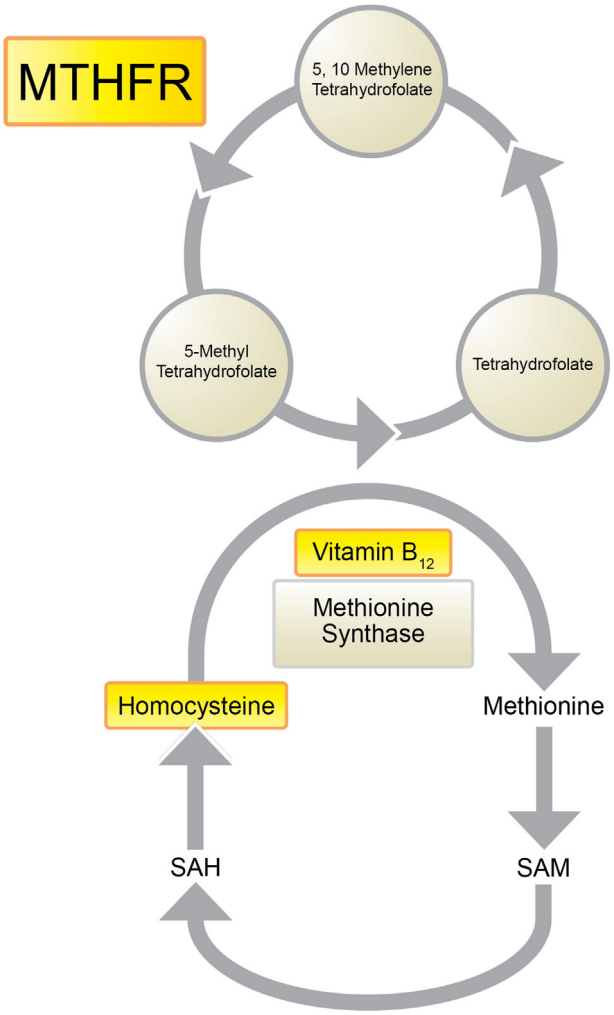

Figure 1. Simplified illustration of the one-carbon cycle. MTHFR, methylenetetrahydrofolate reductase; SAH, S-adenosyl-L-homocysteine; SAM, S-adenosyl-L-methionine.

performance and reduced medial orbitofrontal volumes were significant predictors of depressed mood and tested the hypothesis that compromised integrity in this brain region involved in the cognitive control of emotion may partially explain the relationship between cognitive impairment and depressive symptoms.

METHODS AND MATERIALS

Subjects

We analyzed a large sample of elderly individuals from the Alzheimer's Disease Neuroimaging Initiative (ADNI). The study was conducted according to the Good Clinical Practice guidelines, the Declaration of Helsinki, and U.S. 21 CFR Part 50 (Protection of Human Subjects) and Part 56 (Institutional Review Boards). Written informed consent was obtained from all participants before protocol-specific procedures were performed. All ADNI data are publicly available (http://adni.loni.usc.edu). To avoid the known effects of population stratification on genetic analysis (18), we included only non-Hispanic Caucasian subjects identified by self-report and confirmed by multidimensional scaling analysis (19). The ADNI cohort included multiple diagnostic groups: patients with Alzheimer's disease (AD), subjects with MCI, and healthy elderly (cognitively normal) participants. All subjects were administered the Mini–Mental State Examination (MMSE) (20) and the 15-item version of the Geriatric Depression Scale (GDS-15) (21). Our final analysis comprised 738 individuals (average age ± SD = 75.53 ± 6.78 years; 438 men, 300 women), including 173 AD, 359 MCI, and 206 healthy older adults. All participants received premortem clinical diagnoses, as described in detail in ADNI's General Procedures Manual (http://adni.loni.usc.edu/wp-content/uploads/2010/09/ADNI_GeneralProceduresManual.pdf). Table 1 illustrates demographic, cognitive, and mood data for all participants, stratified by genotype and substratified by diagnostic groups.

Genotyping and Allele Frequency

The ADNI sample was genotyped using the Illumina 610-Quad BeadChip (Illumina, Inc., San Diego, CA). The only polymorphism examined in this study was the C677T functional variant in the *MTHFR* gene, at the rs1801133 locus. Allele frequency was computed from genotype frequency. Distributions of allele frequencies by diagnostic groups were evaluated by χ^2 tests with a .05 significance level, using 3 × 2 and 2 × 2 contingency tables in SPSS, version 23.0 (IBM Corp., Armonk, NY).

Neuroimaging

Whole-Brain Analyses: Tensor-Based Morphometry. The C677T polymorphism was analyzed for association with regional brain volumes in ADNI participants, as detailed below. Subjects were scanned using a standardized MRI protocol developed for this cohort (22,23). Briefly, high-resolution structural brain magnetic resonance images were acquired at 58 sites across North America, using 1.5T MRI scanners. A sagittal three-dimensional magnetization-prepared rapid gradient-echo sequence was used, optimized for consistency across sites (23) (repetition time/echo time = 2400/1000 ms; flip angle = 8°; field of view = 24 cm; final reconstructed voxel resolution = 0.9375 × 0.9375 × 1.2 mm^3). Image corrections were applied using a processing pipeline at the Mayo Clinic, consisting of 1) a procedure termed GradWarp to correct geometric distortion due to gradient nonlinearity (24), 2) a "B1-correction" to adjust for image intensity inhomogeneity due to B1 nonuniformity using calibration scans (23), 3) "N3" bias field correction for reducing residual intensity inhomogeneity (25), and 4) geometrical scaling, according to a phantom scan acquired for each subject (23), to adjust for scanner- and session-specific calibration errors. To adjust for global differences in brain positioning and scale, all subjects' scans were linearly registered to the stereotaxic space defined by the International Consortium for Brain Mapping template (ICBM-53) (26) using a nine-parameter transformation (three translations, three rotations, three scales) (27). We used standard trilinear interpolation and resampled the resulting aligned scans to have 1-mm isotropic voxels.

Table 1. Demographic Data by Diagnostic and C677T Genotype Groups ($N = 738$)

		CC	CT	TT	Total	Group Comparisons
CON	*n*	84 (37 F)	96 (45 F)	26 (12 F)	206 (94 F)	$p = .929$
	Age, years	75.95 ± 4.75 [76]	75.98 ± 5.00 [75]	77.42 ± 5.59 [77]	76.15 ± 4.98 [76]	$p = .380$
	MMSE	29.25 ± 0.94 [30]	29.08 ± 0.99 [29]	29.08 ± 0.85 [29]	29.15 ± 0.95 [29]	$p = .464$
	GDS-15	1.06 ± 1.25 [1]	0.68 ± 1.14 [0]	0.92 ± 0.89 [1]	0.86 ± 1.17 [0]	$p = .089$
MCI	*n*	149 (57 F)	157 (54 F)	53 (17 F)	359 (128 F)	$p = .656$
	Age, years	75.27 ± 6.88 [76]	75.02 ± 7.50 [76]	75.15 ± 7.45 [74]	75.14 ± 7.22 [76]	$p = .957$
	MMSE	26.96 ± 1.74 [27]	27.06 ± 1.83 [27]	27.55 ± 1.75 [28]	27.09 ± 1.78 [27]	$p = .115$
	GDS-15	1.58 ± 1.29 [1]	1.59 ± 1.42 [1]	1.28 ± 1.28 [1]	1.54 ± 1.35 [1]	$p = .330$
AD	*n*	81 (40 F)	67 (25 F)	25 (13 F)	173 (78 F)	$p = .256$
	Age, years	75.04 ± 7.69 [76]	75.91 ± 7.30 [77]	76.48 ± 8.34 [77]	75.58 ± 7.61 [77]	$p = .644$
	MMSE	23.33 ± 1.88 [23]	23.45 ± 2.22 [24]	23.24 ± 1.81 [23]	23.36 ± 2.00 [23]	$p = .892$
	GDS-15	1.64 ± 1.42 [1]	1.58 ± 1.35 [1]	1.84 ± 1.55 [1]	1.65 ± 1.40 [1]	$p = .737$
Total	*n*	314 (134 F)	320 (124 F)	104 (42 F)	738 (300 F)	$p = .602$
	Age, years	75.39 ± 6.61 [76]	75.50 ± 6.80 [76]	76.04 ± 7.26 [77]	75.53 ± 6.78 [76]	$p = .697$
	MMSE	26.64 ± 2.70 [27]	26.91 ± 2.63 [27]	26.89 ± 2.67 [28]	26.79 ± 2.66 [27]	$p = .399$
	GDS-15	1.50 ± 1.33 [1]	1.31 ± 1.39 [1]	1.33 ± 1.30 [1]	1.38 ± 1.35 [1]	$p = .382$

n indicates sample sizes, followed by the number of women in parentheses. Average age, MMSE, and GDS-15 scores are followed by SDs. Median values are indicated in brackets. *p* values for Pearson χ^2 tests (for sex) or one-way analyses of variance (for age, MMSE, and GDS-15 scores) are reported in the last column.

AD, Alzheimer's disease; CON, healthy controls; F, female; GDS-15, 15-item version of the Geriatric Depression Scale; MCI, mild cognitive impairment; MMSE, Mini–Mental State Examination.

We then created a minimal deformation target, which serves as an unbiased average template image for automated image registration and serves to reduce statistical bias. The minimal deformation target was created from the magnetic resonance images of 40 randomly selected healthy elderly subjects, as detailed elsewhere (28,29). To quantify three-dimensional patterns of volumetric tissue variations, all individual T1-weighted images were nonlinearly aligned to the template with an inverse-consistent three-dimensional elastic warping technique using a mutual information cost function (30). Consequently, for each subject, a separate Jacobian matrix field was derived from the gradients of the deformation field that aligned that individual brain to the minimal deformation target. The determinant of the local Jacobian matrix was derived from the forward deformation field to characterize local volume differences. Color-coded Jacobian determinants were used to illustrate regions of volume expansion, that is, those with det J(r) > 1, or contraction, that is, det J(r) < 1 (31–34) relative to the group template. Because all images were registered to the same study-specific template, these Jacobian maps shared common anatomical coordinates, defined by the normal template. Individual Jacobian maps were retained for further statistical analyses.

To model effects of the C677T functional variant in *MTHFR* on local brain volumes, we used univariate linear regression to associate the number of minor T alleles (0, 1, or 2) with the Jacobian values (describing the amount of brain tissue deficit or excess relative to the standard template) at each voxel in the brain, after controlling for age, sex, and diagnosis. To minimize type I errors, we used a searchlight method for false discovery rate correction (35), which controls the false discovery rate in all reported statistical maps. We implemented this method to correct the maps of statistical associations between the image phenotype (morphometry) and genotype at the rs1801133 locus (number of T alleles). All maps shown were thresholded at the appropriate corrected *p* value, after performing searchlight false discovery rate ($q = 0.05$), to show only regions of significance that passed the multiple comparisons correction.

Region of Interest Analyses: Medial Orbitofrontal Volumes. Five MRI core analysis laboratories have provided feature extraction and numeric summaries from the high-quality ADNI MRI data, which are publicly available in the ADNI data archive (http://adni.loni.usc.edu). One of these core analysis laboratories, the Center for Imaging of Neurodegenerative Diseases at the University of California, San Francisco (co-investigator: Norbert Schuff), has provided volumetric segmentation using the FreeSurfer image analyses suite, which is documented and freely available for download online (http://surfer.nmr.mgh.harvard.edu/). Version 4.3 is used for ADNI's cross-sectional data. The input for ADNI FreeSurfer is a T1-weighted image in Neuroimaging Informatics Technology Initiative (NiFTI) format, which has been preprocessed (gradient warping, scaling, B1 correction, and N3 inhomogeneity correction) by the Mayo Clinic preprocessing stream as described above.

Briefly, FreeSurfer processing includes motion correction, removal of nonbrain tissue using a hybrid watershed/surface deformation procedure (36), automated Talairach transformation, segmentation of the subcortical white matter and deep gray matter (37,38), intensity normalization (25), tessellation of the gray matter/white matter boundary, automated topology correction (39,40), and surface deformation following intensity gradients to optimally place the gray/white and gray/cerebrospinal fluid borders at the location where the greatest shift in intensity defines the transition to the other tissue class (41–43), followed by rigorous quality control procedures that allow for

the exclusion of failed segmentations due to poor image quality, registration issues, or processing errors. We downloaded the numeric summaries for "medial orbital frontal" volumes and retained the data pertaining to subjects with frontal segmentations that satisfied all quality control requirements. We obtained the volumes of the medial orbitofrontal cortices (in cubic millimeters) for 640 of our participants.

Blood-Based Markers

In the ADNI public database, plasma homocysteine levels were available for 732 of our participants, 634 of whom also had usable medial orbitofrontal volumes. The database also contained plasma vitamin B_{12} concentrations for 680 of our subjects (including 675 with available homocysteine levels and 587 with both homocysteine and medial orbitofrontal volume data). Homocysteine and vitamin B_{12} levels (in picograms per milliliter) were extracted from blood samples collected via standard venipuncture protocols. Vitamin B_{12} deficiency was defined as plasma levels < 250 pg/mL.

Statistical Analyses

To ensure consistency, we used an additive model of minor T-allele effects—the number of T alleles carried by each participant was coded as 0, 1, or 2—in all analyses aimed at testing the association between the C677T variant and another variable. However, because medial orbitofrontal volumes seemed to be affected in a recessive manner, we additionally ran every regression model using a recessive model of minor allele effects (i.e., comparing C-allele carriers with T homozygotes). These analyses produced similar results, which are presented in Supplemental Tables S2–S4.

We used general linear models to examine the predictors of medial orbitofrontal volumes, plasma homocysteine concentrations, and GDS-15 scores. Shapiro-Wilk tests showed that medial orbitofrontal volumes were normally distributed ($p = .601$), but homocysteine levels ($p < .001$) and GDS-15 scores ($p < .001$) were not. We therefore used standardized scores in all regression models including plasma homocysteine levels or mood scores as the dependent variable. Age and sex were included as covariates in all analyses. We also controlled for diagnosis, except when MMSE score was used as a factor in the model, because MMSE scores are one of the major diagnostic criteria for dementia, as described in ADNI's General Procedures Manual (http://adni.loni.usc.edu/wp-content/uploads/2010/09/ADNI_GeneralProceduresManual.pdf). These statistical analyses were conducted in SPSS, version 23.0.

Simple mediation analyses were conducted using Andrew Hayes's PROCESS Procedure (version 2.15) for SPSS (http://www.processmacro.org/download.html). We obtained path coefficients (a, b, c, and c') representing the linear regression coefficients for each path in the mediation model. We standardized all variables to facilitate the interpretation of path coefficients, now bounded by -1 and 1 across all measures. The a-path represents the association between the predictor and mediator variables. The b-path denotes the relationship between the mediator and outcome variables, while also controlling for the predictor variable. The c'-path (also called "direct effect") and the c-path (also known as "total effect") represent the associations between the predictor and outcome variables including and excluding the mediator variable, respectively. If the difference between c and c' is statistically significant, there is a significant mediation effect. It was previously shown that $a \times b = c - c'$; therefore, we tested the significance of $a \times b$ (also known as "indirect effect") using bootstrapped confidence intervals (CIs) (44). Bootstrapping creates thousands of simulated datasets using resampling with replacement and runs the analysis once in each simulated sample (45). Of the generated statistics, 95% fall between two values, and if that CI for $a \times b$ does not include 0, a significant ($p < .05$) mediation has occurred. Percent mediation [P_M] is a measure of effect size interpreted as the percent of the total effect (c) accounted for by the indirect effect ($a \times b$); that is, $P_M = (a \times b)/c$ (44).

RESULTS

Consistent with the prevailing view that the *MTHFR* C677T polymorphism may not be a risk factor for AD, but appears to be associated with various types of age-related disorders (46), the distributions of genotype ($p = .592$) and allele frequency ($p = .667$) for rs1801133 did not significantly differ across the three diagnostic groups in the ADNI cohort (Table 2). Nonetheless, this functional variant in *MTHFR* predicted differences in regional brain volumes in our large elderly sample after controlling for age, sex, and diagnosis. As depicted in Figure 2, smaller volumes in the frontal (including the bilateral cingulate gyri, middle frontal gyri, lateral and medial orbitofrontal cortices), parietal (notably the inferior parietal lobule), and temporal lobes (especially the superior temporal gyrus), as well as in the thalamus, were statistically related to carrying the minor T allele at the rs1801133 locus. Strong genotype group differences were also observed in periventricular regions. Each copy of the "risk" allele was associated with a 2% to 4% reduction in local brain volumes (Figure 2).

Table 2. Genotype and Allele Frequency by Diagnostic Groups ($N = 738$)

		CON	MCI	AD	Pearson χ^2 Test
Total	$N = 738$	206	359	173	
Genotype Frequency	CC	84 (41%)	149 (41%)	81 (47%)	$p = .592$
	CT	96 (46%)	157 (44%)	67 (39%)	
	TT	26 (13%)	53 (15%)	25 (14%)	
Allele Frequency	C	264 (64%)	455 (63%)	229 (66%)	$p = .667$
	T	148 (36%)	263 (37%)	117 (34%)	

AD, Alzheimer's disease; CON, healthy controls; MCI, mild cognitive impairment.

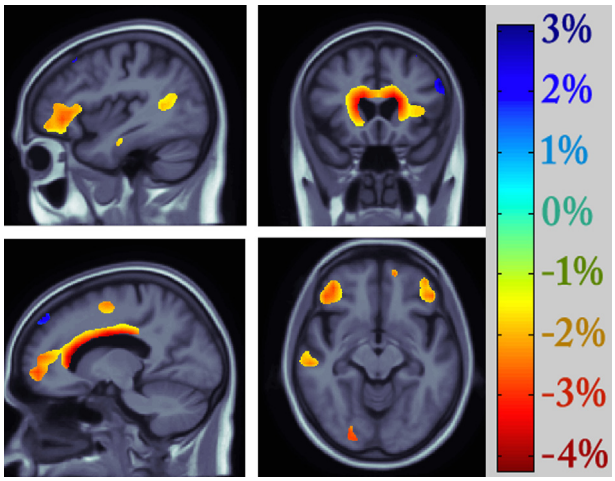

Figure 2. Effects of the C677T variant on regional brain volumes (N = 738). Negative beta values (warm colors) show regions in which each risk T allele was associated with a 2% to 4% volume deficit, as shown on the color bar. Tests for associations are adjusted for age, sex, and diagnosis; maps are corrected for multiple comparisons with the searchlight false discovery rate method at q = 0.05. Images are in radiological convention (left side of the brain shown on the right).

Among the regions showing a significant association with *MTHFR* genotype in our whole-brain analyses, the medial orbitofrontal cortex was particularly noteworthy because of its involvement, not just in mood states and intellectual functioning, but specifically in the cognitive modulation of emotional processes. This brain area therefore was selected as the region of interest in our investigations of the relationships between brain integrity, clinical outcomes, and homocysteine metabolism. Our region of interest analyses, which used FreeSurfer volumes in a subset of the same elderly sample (Supplemental Table S1), confirmed that the C677T variant was associated with reduced medial orbitofrontal volumes (p = .033, F ratio = 3.428) after controlling for age, sex, and diagnosis (Supplemental Table S2). As expected, the C677T variant was also associated with significant elevations in plasma homocysteine levels (p < .001, F ratio = 10.375) after controlling for age, sex, and dementia status (Supplemental Table S2). Mediation analyses further revealed a significant indirect effect of the number of T alleles on medial orbitofrontal volumes through plasma homocysteine levels, $a \times b$ = −0.015 (95% CI, −0.039 to −0.003). The mediator accounted for about one-quarter of the total effect, P_M = 0.253 (Figure 3).

We then tested the hypothesis that the relationship between genotype and plasma homocysteine concentrations may differ between individuals with inadequate circulatory levels of vitamin B_{12} (i.e., who are deficient in a major cofactor used by methionine synthase to remethylate homocysteine into methionine) and nondeficient subjects by introducing vitamin B_{12} deficiency status as a covariate in addition to age, sex, and diagnosis in the regression models. The C677T variant showed even stronger associations with elevations in plasma homocysteine levels (p < .001, F ratio = 12.143), vitamin B_{12} deficiency was an independent predictor of homocysteine concentrations (p = .021, F ratio = 5.348), and the genotype-by-deficiency status interaction term was

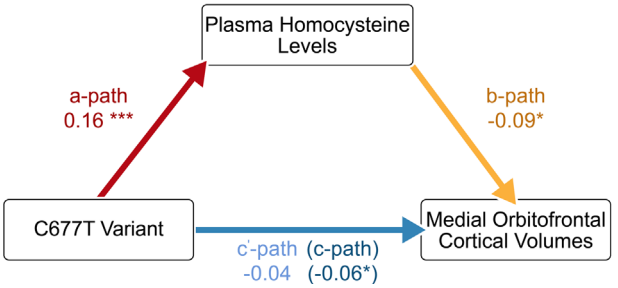

Figure 3. Mediation of the association between genotype and medial orbitofrontal volumes by plasma homocysteine levels (n = 634). Path coefficients for simple mediation analysis using the PROCESS Procedure for SPSS. The *a*-path represents the association between genotype and plasma homocysteine levels. The *b*-path denotes the relationship between plasma homocysteine levels and medial orbitofrontal volumes while also controlling for genotype. The *c*′-path and *c*-path represent the associations between genotype and medial orbitofrontal volumes with and without plasma homocysteine levels included as a mediator, respectively. $^{*}p$ < .05, $^{***}p$ < .001.

significant (p = .011, F ratio = 4.529), supporting our hypothesis (Supplemental Table S3). Within-group analyses confirmed that in vitamin B_{12}–deficient individuals, carrying the allele conferring reduced enzymatic activity was more strongly associated with increased plasma homocysteine concentrations (p = .008, F ratio = 5.122) than in nondeficient subjects (p = .055, F ratio = 2.911) after controlling for age, sex, and dementia status (Supplemental Table S3).

We subsequently examined predictors of GDS-15 scores across the entire sample. We found no significant main effects of the C677T variant (p = .256, F ratio = 1.368), homocysteine levels (p = .823, F ratio = 0.050), or vitamin B_{12} deficiency status (p = .961, F ratio = 0.002) on mood scores. However, cognitive decline, assessed with the MMSE (p < .001,

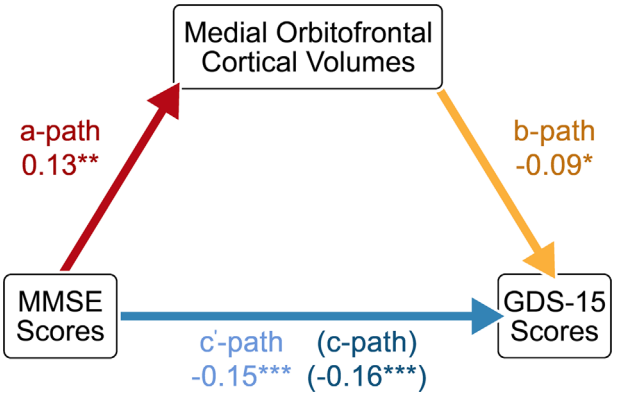

Figure 4. Partial mediation of the association between performance on the Mini-Mental State Examination (MMSE) and scores on the 15-item version of the Geriatric Depression Scale (GDS-15) by medial orbitofrontal volumes (n = 640). Path coefficients for simple mediation analysis using the PROCESS Procedure for SPSS. The *a*-path represents the association between MMSE scores and medial orbitofrontal volumes. The *b*-path denotes the relationship between medial orbitofrontal volumes and GDS scores while also controlling for MMSE performance. The *c*′-path and the *c*-path represent the associations between MMSE and GDS scores with and without medial orbital cortical volumes included as a mediator, respectively. $^{*}p$ < .05, $^{**}p$ < .01, $^{***}p$ < .001.

F ratio = 12.808), and medial orbitofrontal atrophy ($p = .005$, *F* ratio = 7.840) were associated with greater depressive symptoms (i.e., higher GDS-15 scores) after controlling for age and sex (Supplemental Table S4). Further analyses revealed a significant partial mediation of MMSE-GDS associations by medial orbitofrontal volumes, $a \times b = -0.012$ (95% CI, −0.027 to −0.003). The mediator accounted for about 8% of the total effect, $P_M = 0.075$ (Figure 4). These results are summarized in Supplemental Figure S1.

DISCUSSION

The C677T functional variant in *MTHFR* is a risk factor for hyperhomocysteinemia and has been associated with higher rates of various age-related disorders (46). This study expands on our earlier report of a link between the C677T variant and regional brain atrophy in two independent elderly cohorts with MCI (15) by providing evidence for these associations across the spectrum of normal cognitive aging, MCI, and AD. For the first time in this report, we address the mechanisms through which genetic variation in *MTHFR* alters brain integrity and affects mood-cognition associations in the elderly. These novel findings bring together prior work reporting that both the C677T variant (15) and plasma homocysteine levels (13) are significant predictors of reduced regional brain volumes in older adults. These results also suggest the importance of adequate vitamin B_{12} intake, especially in carriers of the thermolabile variant, consistent with a prior report highlighting the significance of this vitamin in relation to homocysteine-induced regional brain atrophy (47).

Whole-brain tensor-based morphometry analyses revealed associations between the C677T variant and reduced volumes in several brain regions involved in intellectual functioning (e.g., the middle frontal gyrus and inferior parietal lobule) and in the regulation of emotional and cognitive aspects of goal-directed behavior (e.g., the superior temporal gyrus, cingulate gyrus, and orbitofrontal cortex). In particular, the medial orbitofrontal cortex is a functionally complex structure with extensive projections to and from primary sensory cortices, different prefrontal regions and other association areas, limbic structures, and the medial temporal lobe. It is implicated in high-level aspects of cognition and mediates important aspects of emotional behavior. Notably, converging evidence from multiple lines of study suggests its involvement in the cognitive modulation of the affective and reward value of stimuli and emotion-related states (48).

Medial orbitofrontal atrophy occurs early in the course of dementia (49,50), and structural abnormalities in this region have been associated with depressive symptoms in both middle-aged (51) and geriatric (52–54) subjects. In fact, the largest ever and most recent worldwide meta-analysis of cortical thickness reductions in depressed patients relative to controls reported the largest effect sizes in medial orbitofrontal cortices (55). Cognitive decline in the elderly is frequently accompanied by depressed mood (56,57), and neurodegeneration appears to play an important role in the pathogenesis of depression associated with cognitive concerns (58). Here, we examined predictors of mood scores and found that the only two variables significantly associated with depressive symptoms were medial orbitofrontal atrophy and cognitive impairment. We also uncovered a significant mediation of these mood-cognition associations by medial orbitofrontal volumes, thereby integrating findings from multiple prior studies.

Our tensor-based morphometry analyses also showed significant associations between the C677T variant and reduced volumes in periventricular regions. A decrease in the size of periventricular structures allows the ventricles to expand; thus, this finding appears consistent with prior reports of an association between plasma homocysteine level and ventricular enlargement in older adults (59,60). However, this result should be interpreted with caution. Movement artifacts are sometimes more evident at tissue interfaces where changes in signal intensity are most pronounced, such as along the brain–cerebrospinal fluid border, and head motion during MRI acquisition can also tend to reduce gray matter volume and thickness estimates (61). Moreover, participant motion is increased in elderly and clinical populations (62), and most image processing methods combined with the exclusion of low-quality scans based on visual inspection are not always sufficient to fully account for motion as a confounding variable (61). Therefore, despite the rigorous motion correction and quality control procedures implemented in this study, we cannot exclude the possibility that the periventricular volume differences we observed may be due in part to greater head motion.

Carriers of the T allele have higher plasma homocysteine concentrations, as evidenced by multiple genome-wide association studies (63–67). Homocysteine is prothrombotic and proatherogenic, resulting in damage to vessel walls. It is also toxic to neurons by multiple mechanisms, including inflammation and pro-oxidation, direct DNA damage, and glutamate excitotoxicity (68). Elevated homocysteine levels have been associated with brain atrophy in the elderly, which may be due to the cerebrovascular as well as the direct neurotoxic effects of this amino acid. Notably, we showed that higher plasma homocysteine levels predicted regional brain volume deficits in older adults (13), and the present study suggests that our previously reported associations between the C677T variant and more pronounced brain atrophy in MCI (15) also apply to patients with dementia and healthy older adults. Here, we additionally show that the effect of this polymorphism on medial orbitofrontal volumes is mediated by increased plasma homocysteine levels, which further elucidates a possible causal pathway between *MTHFR* genotype and brain tissue loss in the elderly.

Our results also suggest that vitamin B_{12} deficiency interacts with the C677T variant in the etiology of hyperhomocysteinemia and associated disorders. Although it may be possible to offset the pathogenic effects of certain variants by dietary supplementation, our findings imply that the same interventions may be ineffective in individuals who do not carry these variants. This provides a potential explanation for the discrepancies reported in studies evaluating the efficacy of supplementation with B vitamins (69). The metabolism of homocysteine is complex; thus, stratifying participants by genetic and physiological risk factors for hyperhomocysteinemia—or a combined risk index based on genetic, imaging, and peripheral blood markers—may allow for more sensitive and focused future clinical trials of degenerative brain diseases

and age-related disorders. Furthermore, because high intake of B vitamins can have detrimental effects in some individuals (70), this report also highlights the importance of personalized medicine in determining appropriate levels of B vitamin intake and underscores the need for novel approaches to reducing plasma homocysteine concentrations [e.g., by enhancing the conversion of this amino acid to cysteine in the liver or by supporting its urinary excretion (71)].

Since the Alzheimer's Disease Neuroimaging Initiative was established in 2004, more than 500 studies of the ADNI dataset have been published and have resulted in numerous major accomplishments (72). Notably, following the identification of novel genetic risk factors for age-related disorders, many studies have focused on associations between these risk variants and brain measures. These include our prior reports of the effects of Alzheimer's risk variants in *APOE* and *CLU* on ventricular expansion rate (73) and obesity-related polymorphism in *FTO* on regional brain atrophy (74). An important insight from this line of study was the understanding that genetic risk factors affect the trajectory of brain aging even in cognitively normal individuals. Another area of focus in research using ADNI data has been the elucidation of relationships between blood metabolite levels and various imaging, genetic, and clinical correlates. Examples include our prior studies of associations between plasma leptin levels and brain volumes (75) and between serum cholesterol levels, a cholesterol-related gene, and white matter microstructure (76). This line of study has led to a better understanding of the link between different biomarkers associated with aging and neurodegenerative disorders.

The present report goes one step further and proposes a mechanistic model of the relationships among three clusters of information: homocysteine metabolism (*MTHFR* genotype, vitamin B_{12} deficiency, plasma homocysteine concentrations), regional brain volumes, and clinical symptoms (MMSE and GDS-15 scores). We found that the association between the C677T variant and reduced volumes of medial orbitofrontal cortices was mediated by increased plasma homocysteine levels, and that the link between cognitive impairment and depressive symptoms was partially mediated by decreased medial orbitofrontal volumes, suggesting that this functional variant may affect the relationship between cognitive decline and depressed mood in older adults, perhaps through its effect on regional atrophy in brain regions involved in the cognitive modulation of emotional processes.

Future studies are needed to provide a validation of these models in different elderly cohorts. It is also important for future investigations to address how this genetic variant interacts with other polymorphisms [especially variants that also confer a predisposition to hyperhomocysteinemia, such as those in the *ZNF366* and *PTPRD* genes (64)] and with environmental factors (including vitamin deficiencies, alcohol consumption, and therapeutic drug use) to affect the trajectory of brain aging, and indirectly, intellectual and emotional functioning in older adults. Nonetheless, by modeling some of the mechanisms through which the C677T variant affects regional brain volumes and how these changes relate to cognitive impairment and depressive symptoms across the spectrum of healthy aging, MCI, and AD, this study represents an important advance in our understanding of clinically relevant associations relating to this widely studied polymorphism in *MTHFR*.

ACKNOWLEDGMENTS AND DISCLOSURES

This work was supported in part by a Turken Research Award from the Sam and Ida Turken Charitable Foundation (to FFR), a training grant from the National Institute of Neurological Disorders and Stroke of the National Institutes of Health (Grant No. T32NS048004 to FFR); and additional grants from the National Institutes of Health (Grant Nos. R01 MH097268, R01 AG040060 to PMT). Data collection and sharing for this project was funded by the Alzheimer's Disease Neuroimaging Initiative (ADNI) (National Institutes of Health Grant No. U01 AG024904). ADNI is funded by the National Institute on Aging, the National Institute of Biomedical Imaging and Bioengineering, and through generous contributions from the following: Alzheimer's Association; Alzheimer's Drug Discovery Foundation; BioClinica, Inc.; Biogen Idec Inc.; Bristol-Myers Squibb Company; Eisai Inc.; Elan Pharmaceuticals, Inc.; Eli Lilly and Company; F. Hoffmann-La Roche Ltd. and its affiliated company Genentech, Inc.; GE Healthcare; Innogenetics, N.V.; IXICO Ltd.; Janssen Alzheimer Immunotherapy Research & Development, LLC; Johnson & Johnson Pharmaceutical Research & Development, LLC; Medpace, Inc.; Merck & Co., Inc.; Meso Scale Diagnostics, LLC; NeuroRx Research; Novartis Pharmaceuticals Corporation; Pfizer Inc.; Piramal Imaging; Servier; Synarc Inc.; and Takeda Pharmaceutical Company. The Canadian Institutes of Health Research is providing funds to support ADNI clinical sites in Canada. Private sector contributions are facilitated by the Foundation for the National Institutes of Health (www.fnih.org). The grantee organization is the Northern California Institute for Research and Education, and the study is coordinated by the Alzheimer's Disease Cooperative Study at the University of California, San Diego. ADNI data are disseminated by the Laboratory for Neuro Imaging at the University of Southern California.

Data used in preparation of this article were obtained from the ADNI database (adni.loni.usc.edu). As such, the investigators within the ADNI contributed to the design and implementation of ADNI and/or provided data but did not participate in analysis or writing of this report. A complete listing of ADNI investigators can be found at: adni.loni.usc.edu/wp-content/uploads/how_to_apply/ADNI_Acknowledgement_List.pdf.

All authors report no biomedical financial interests or potential conflicts of interest.

ARTICLE INFORMATION

From the Departments of Neurology (FFR, KLN, PMT) and Psychiatry (GWS, PMT), Semel Institute, David Geffen School of Medicine at UCLA; and Imaging Genetics Center (FFR, XH, PMT) and Departments of Neurology (XH, PMT), Psychiatry (PMT), Radiology (PMT), Engineering (PMT), Pediatrics (PMT), and Ophthalmology (PMT), Keck School of Medicine, University of Southern California, Los Angeles, California.

Address correspondence to Florence F. Roussotte, Ph.D., Department of Neurology, 635 Charles E. Young Drive South, Neuroscience Research Building (NRB) Suite 225, Los Angeles, CA 90095; E-mail: florence78@ucla.edu.

Received Aug 17, 2016; revised and accepted Sep 15, 2016.

Supplementary material cited in this article is available online at http://dx.doi.org/10.1016/j.bpsc.2016.09.005.

REFERENCES

1. Cattaneo M (1999): Hyperhomocysteinemia, atherosclerosis and thrombosis. Thromb Haemost 81:165–176.
2. Zhou J, Austin RC (2009): Contributions of hyperhomocysteinemia to atherosclerosis: Causal relationship and potential mechanisms. Biofactors 35:120–129.
3. McIlroy SP, Dynan KB, Lawson JT, Patterson CC, Passmore AP (2002): Moderately elevated plasma homocysteine, methylenetetrahydrofolate reductase genotype, and risk for stroke, vascular dementia, and Alzheimer disease in Northern Ireland. Stroke 33:2351–2356.

4. Hainsworth AH, Yeo NE, Weekman EM, Wilcock DM (2016): Homocysteine, hyperhomocysteinemia and vascular contributions to cognitive impairment and dementia (VCID). Biochim Biophys Acta 1862: 1008–1017.
5. Budge MM, de Jager C, Hogervorst E, Smith AD; Oxford Project to Investigate Memory and Ageing (OPTIMA). (2002): Total plasma homocysteine, age, systolic blood pressure, and cognitive performance in older people. J Am Geriatr Soc 50:2014–2018.
6. Riggs KM, Spiro A 3rd, Tucker K, Rush D (1996): Relations of vitamin B-12, vitamin B-6, folate, and homocysteine to cognitive performance in the Normative Aging Study. Am J Clin Nutr 63:306–314.
7. Lehmann M, Gottfries CG, Regland B (1999): Identification of cognitive impairment in the elderly: Homocysteine is an early marker. Dementia Geriatr Cogn Disord 10:12–20.
8. Duthie SJ, Whalley LJ, Collins AR, Leaper S, Berger K, Deary IJ (2002): Homocysteine, B vitamin status, and cognitive function in the elderly. Am J Clin Nutr 75:908–913.
9. Agrawal A, Ilango K, Singh PK, Karmakar D, Singh GP, Kumari R, *et al*. (2015): Age dependent levels of plasma homocysteine and cognitive performance. Behav Brain Res 283:139–144.
10. Kim JM, Stewart R, Kim SW, Yang SJ, Shin IS, Yoon JS (2008): Predictive value of folate, vitamin B12 and homocysteine levels in late-life depression. Br J Psychiatry 192:268–274.
11. Bhatia P, Singh N (2015): Homocysteine excess: Delineating the possible mechanism of neurotoxicity and depression. Fundam Clin Pharmacol 29:522–528.
12. Almeida OP, McCaul K, Hankey GJ, Norman P, Jamrozik K, Flicker L (2008): Homocysteine and depression in later life. Arch Gen Psychiatry 65:1286–1294.
13. Rajagopalan P, Hua X, Toga AW, Jack CR Jr, Weiner MW, Thompson PM (2011): Homocysteine effects on brain volumes mapped in 732 elderly individuals. Neuroreport 22:391–395.
14. Madsen SK, Rajagopalan P, Joshi SH, Toga AW, Thompson PM; Alzheimer's Disease Neuroimaging Initiative. (2015): Higher homocysteine associated with thinner cortical gray matter in 803 participants from the Alzheimer's Disease Neuroimaging Initiative. Neurobiol Aging 36(suppl 1):S203–S210.
15. Rajagopalan P, Jahanshad N, Stein JL, Hua X, Madsen SK, Kohannim O, *et al*. (2012): Common folate gene variant, MTHFR C677T, is associated with brain structure in two independent cohorts of people with mild cognitive impairment. Neuroimage Clin 1: 179–187.
16. Sheweita SA, Baghdadi H, Allam AR (2011): Role of genetic changes in the progression of cardiovascular diseases. Int J Biomed Sci 7: 238–248.
17. da Costa AL, Santos Varela J, Mazetti O, Restelatto L, Fitterman CA, Godinho C, *et al*. (2008): Comparison of the Mini Mental State Examination and depressive symptoms between high cardiovascular risk and healthy community elderly groups. Dementia Neuropsychol 2:294–299.
18. Lander ES, Schork NJ (1994): Genetic dissection of complex traits. Science 265:2037–2048.
19. Stein JL, Hua X, Morra JH, Lee S, Hibar DP, Ho AJ, *et al*. (2010): Genome-wide analysis reveals novel genes influencing temporal lobe structure with relevance to neurodegeneration in Alzheimer's disease. Neuroimage 51:542–554.
20. Folstein MF, Folstein SE, McHugh PR (1975): "Mini-mental state". A practical method for grading the cognitive state of patients for the clinician. J Psychiatr Res 12:189–198.
21. Almeida OP, Almeida SA (1999): Short versions of the Geriatric Depression Scale: A study of their validity for the diagnosis of a major depressive episode according to ICD-10 and DSM-IV. Int J Geriatr Psychiatry 14:858–865.
22. Leow AD, Klunder AD, Jack CR Jr, Toga AW, Dale AM, Bernstein MA, *et al*. (2006): Longitudinal stability of MRI for mapping brain change using tensor-based morphometry. Neuroimage 31:627–640.
23. Jack CR Jr, Bernstein MA, Fox NC, Thompson P, Alexander G, Harvey D, *et al*. (2008): The Alzheimer's Disease Neuroimaging Initiative (ADNI): MRI methods. J Magn Reson Imaging 27:685–691.
24. Jovicich J, Czanner S, Greve D, Haley E, van der Kouwe A, Gollub R, *et al*. (2006): Reliability in multi-site structural MRI studies: Effects of gradient non-linearity correction on phantom and human data. Neuroimage 30:436–443.
25. Sled JG, Zijdenbos AP, Evans AC (1998): A nonparametric method for automatic correction of intensity nonuniformity in MRI data. IEEE Trans Med Imaging 17:87–97.
26. Mazziotta J, Toga A, Evans A, Fox P, Lancaster J, Zilles K, *et al*. (2001): A probabilistic atlas and reference system for the human brain: International Consortium for Brain Mapping (ICBM). Philos Trans R Soc Lond B Biol Sci 356:1293–1322.
27. Collins DL, Neelin P, Peters TM, Evans AC (1994): Automatic 3D intersubject registration of MR volumetric data in standardized Talairach space. J Comput Assist Tomogr 18:192–205.
28. Hua X, Leow AD, Lee S, Klunder AD, Toga AW, Lepore N, *et al*. (2008): 3D characterization of brain atrophy in Alzheimer's disease and mild cognitive impairment using tensor-based morphometry. Neuroimage 41:19–34.
29. Hua X, Leow AD, Parikshak N, Lee S, Chiang MC, Toga AW, *et al*. (2008): Tensor-based morphometry as a neuroimaging biomarker for Alzheimer's disease: An MRI study of 676 AD, MCI, and normal subjects. Neuroimage 43:458–469.
30. Leow A, Huang SC, Geng A, Becker J, Davis S, Toga A, Thompson P (2005): Inverse consistent mapping in 3D deformable image registration: Its construction and statistical properties. Inf Process Med Imaging 19:493–503.
31. Freeborough PA, Fox NC (1998): Modeling brain deformations in Alzheimer disease by fluid registration of serial 3D MR images. J Comput Assist Tomogr 22:838–843.
32. Thompson PM, Giedd JN, Woods RP, MacDonald D, Evans AC, Toga AW (2000): Growth patterns in the developing brain detected by using continuum mechanical tensor maps. Nature 404:190–193.
33. Chung MK, Worsley KJ, Paus T, Cherif C, Collins DL, Giedd JN, *et al*. (2001): A unified statistical approach to deformation-based morphometry. Neuroimage 14:595–606.
34. Riddle WR, Li R, Fitzpatrick JM, DonLevy SC, Dawant BM, Price RR (2004): Characterizing changes in MR images with color-coded Jacobians. Magn Reson Imaging 22:769–777.
35. Langers DR, Jansen JF, Backes WH (2007): Enhanced signal detection in neuroimaging by means of regional control of the global false discovery rate. Neuroimage 38:43–56.
36. Segonne F, Dale AM, Busa E, Glessner M, Salat D, Hahn HK, *et al*. (2004): A hybrid approach to the skull stripping problem in MRI. Neuroimage 22:1060–1075.
37. Fischl B, Salat DH, Busa E, Albert M, Dieterich M, Haselgrove C, *et al*. (2002): Whole brain segmentation: Automated labeling of neuroanatomical structures in the human brain. Neuron 33:341–355.
38. Fischl B, Salat DH, van der Kouwe AJ, Makris N, Segonne F, Quinn BT, *et al*. (2004): Sequence-independent segmentation of magnetic resonance images. Neuroimage 23(suppl 1):S69–S84.
39. Fischl B, Liu A, Dale AM (2001): Automated manifold surgery: Constructing geometrically accurate and topologically correct models of the human cerebral cortex. IEEE Trans Med Imaging 20:70–80.
40. Segonne F, Pacheco J, Fischl B (2007): Geometrically accurate topology-Correction of cortical surfaces using nonseparating loops. IEEE Trans Med Imaging 26:518–529.
41. Dale AM, Fischl B, Sereno MI (1999): Cortical surface-based analysis. I. Segmentation and surface reconstruction. Neuroimage 9:179–194.
42. Dale AM, Sereno MI (1993): Improved localizadon of cortical activity by combining EEG and MEG with MRI cortical surface reconstruction: A linear approach. J Cogn Neurosci 5:162–176.
43. Fischl B, Dale AM (2000): Measuring the thickness of the human cerebral cortex from magnetic resonance images. Proc Natl Acad Sci U S A 97:11050–11055.
44. Hayes AF (2013): Introduction to Mediation, Moderation, and Conditional Process Analysis: A Regression-Based Approach. New York: Guilford Press.
45. Hesterberg T, Monaghan S, Moore DS, Clipson A, Epstein R (2003): Bootstrap Methods and Permutation Tests. New York: W.H. Freeman.

46. Liew SC, Gupta ED (2015): Methylenetetrahydrofolate reductase (MTHFR) C677T polymorphism: Epidemiology, metabolism and the associated diseases. Eur J Med Genet 58:1–10.
47. Douaud G, Refsum H, de Jager CA, Jacoby R, Nichols TE, Smith SM, *et al*. (2013): Preventing Alzheimer's disease-related gray matter atrophy by B-vitamin treatment. Proc Natl Acad Sci U S A 110:9523–9528.
48. Rolls ET, Grabenhorst F (2008): The orbitofrontal cortex and beyond: From affect to decision-making. Prog Neurobiol 86:216–244.
49. Prestia A, Baglieri A, Pievani M, Bonetti M, Rasser PE, Thompson PM, *et al*. (2013): The in vivo topography of cortical changes in healthy aging and prodromal Alzheimer's disease. Suppl Clin Neurophysiol 62:67–80.
50. Pini L, Pievani M, Bocchetta M, Altomare D, Bosco P, Cavedo E, *et al*. (2016): Brain atrophy in Alzheimer's disease and aging. Ageing Res Rev 30:25–48.
51. Bremner JD, Vythilingam M, Vermetten E, Nazeer A, Adil J, Khan S, *et al*. (2002): Reduced volume of orbitofrontal cortex in major depression. Biol Psychiatry 51:273–279.
52. Lee SH, Payne ME, Steffens DC, McQuoid DR, Lai TJ, Provenzale JM, *et al*. (2003): Subcortical lesion severity and orbitofrontal cortex volume in geriatric depression. Biol Psychiatry 54:529–533.
53. Taylor WD, Macfall JR, Payne ME, McQuoid DR, Steffens DC, Provenzale JM, *et al*. (2007): Orbitofrontal cortex volume in late life depression: influence of hyperintense lesions and genetic polymorphisms. Psychol Med 37:1763–1773.
54. Ribeiz SR, Duran F, Oliveira MC, Bezerra D, Castro CC, Steffens DC, *et al*. (2013): Structural brain changes as biomarkers and outcome predictors in patients with late-life depression: A cross-sectional and prospective study. PloS One 8:e80049.
55. Schmaal L, Hibar DP, Samann PG, Hall GB, Baune BT, Jahanshad N, *et al*. (2016): Cortical abnormalities in adults and adolescents with major depression based on brain scans from 20 cohorts worldwide in the ENIGMA Major Depressive Disorder Working Group [published online ahead of print May 3]. Mol Psychiatry.
56. Wang S, Blazer DG (2015): Depression and cognition in the elderly. Annu Rev Clin Psychol 11:331–360.
57. Morimoto SS, Kanellopoulos D, Manning KJ, Alexopoulos GS (2015): Diagnosis and treatment of depression and cognitive impairment in late life. Ann N Y Acad Sci 1345:36–46.
58. Kim HK, Nunes PV, Oliveira KC, Young LT, Lafer B (2016): Neuropathological relationship between major depression and dementia: A hypothetical model and review. Prog Neuropsychopharmacol Biol Psychiatry 67:51–57.
59. Jochemsen HM, Kloppenborg RP, de Groot LC, Kampman E, Mali WP, van der Graaf Y, *et al*. (2013): Homocysteine, progression of ventricular enlargement, and cognitive decline: The Second Manifestations of ARTerial disease-Magnetic Resonance study. Alzheimers Dement 9:302–309.
60. Feng L, Isaac V, Sim S, Ng TP, Krishnan KR, Chee MW (2013): Associations between elevated homocysteine, cognitive impairment, and reduced white matter volume in healthy old adults. Am J Geriatr Psychiatry 21:164–172.
61. Reuter M, Tisdall MD, Qureshi A, Buckner RL, van der Kouwe AJ, Fischl B (2015): Head motion during MRI acquisition reduces gray matter volume and thickness estimates. Neuroimage 107:107–115.
62. Pardoe HR, Kucharsky Hiess R, Kuzniecky R (2016): Motion and morphometry in clinical and nonclinical populations. Neuroimage 135: 177–185.
63. Hazra A, Kraft P, Lazarus R, Chen C, Chanock SJ, Jacques P, *et al*. (2009): Genome-wide significant predictors of metabolites in the one-carbon metabolism pathway. Hum Mol Genet 18:4677–4687.
64. Malarstig A, Buil A, Souto JC, Clarke R, Blanco-Vaca F, Fontcuberta J, *et al*. (2009): Identification of ZNF366 and PTPRD as novel determinants of plasma homocysteine in a family-based genome-wide association study. Blood 114:1417–1422.
65. Pare G, Chasman DI, Parker AN, Zee RR, Malarstig A, Seedorf U, *et al*. (2009): Novel associations of CPS1, MUT, NOX4, and DPEP1 with plasma homocysteine in a healthy population: A genome-wide evaluation of 13 974 participants in the Women's Genome Health Study. Circ Cardiovasc Genet 2:142–150.
66. Tanaka T, Scheet P, Giusti B, Bandinelli S, Piras MG, Usala G, *et al*. (2009): Genome-wide association study of vitamin B6, vitamin B12, folate, and homocysteine blood concentrations. Am J Hum Genet 84:477–482.
67. Lange LA, Croteau-Chonka DC, Marvelle AF, Qin L, Gaulton KJ, Kuzawa CW, *et al*. (2010): Genome-wide association study of homocysteine levels in Filipinos provides evidence for CPS1 in women and a stronger MTHFR effect in young adults. Hum Mol Genet 19:2050–2058.
68. Sachdev PS (2005): Homocysteine and brain atrophy. Prog Neuropsychopharmacol Biol Psychiatry 29:1152–1161.
69. Morris MS (2012): The role of B vitamins in preventing and treating cognitive impairment and decline. Adv Nutr 3:801–812.
70. Shorter KR, Felder MR, Vrana PB (2015): Consequences of dietary methyl donor supplements: Is more always better? Prog Biophys Mol Biol 118:14–20.
71. Loscalzo J (2006): Homocysteine trials–Clear outcomes for complex reasons. N Engl J Med 354:1629–1632.
72. Weiner MW, Veitch DP, Aisen PS, Beckett LA, Cairns NJ, Cedarbaum J, *et al*. (2015): 2014 Update of the Alzheimer's Disease Neuroimaging Initiative: A review of papers published since its inception. Alzheimers Dement 11:e1–120.
73. Roussotte FF, Gutman BA, Madsen SK, Colby JB, Thompson PM; Alzheimer's Disease Neuroimaging Initiative. (2014): Combined effects of Alzheimer risk variants in the CLU and ApoE genes on ventricular expansion patterns in the elderly. J Neurosci 34: 6537–6545.
74. Ho AJ, Stein JL, Hua X, Lee S, Hibar DP, Leow AD, *et al*. (2010): A commonly carried allele of the obesity-related FTO gene is associated with reduced brain volume in the healthy elderly. Proc Natl Acad Sci U S A 107:8404–8409.
75. Rajagopalan P, Toga AW, Jack CR, Weiner MW, Thompson PM; Alzheimer's Disease Neuroimaging Initiative. (2013): Fat-mass-related hormone, plasma leptin, predicts brain volumes in the elderly. Neuroreport 24:58–62.
76. Warstadt NM, Dennis EL, Jahanshad N, Kohannim O, Nir TM, McMahon KL, *et al*. (2014): Serum cholesterol and variant in cholesterol-related gene CETP predict white matter microstructure. Neurobiol Aging 35:2504–2513.